J|A|C|S ARTICLES

Published on Web 05/13/2009

Multiple Modes for Coordination of Phenazine to Molybdenum: Ring Fusion Promotes Access to η^4-Coordination, Oxidative Addition of Dihydrogen and Hydrogenation of Aromatic Nitrogen Compounds

Aaron Sattler, Guang Zhu, and Gerard Parkin*

Department of Chemistry, Columbia University, New York, New York 10027

Received March 11, 2009; E-mail: parkin@columbia.edu

Abstract: $Mo(PMe_3)_6$ reacts with phenazine (PhzH) to give (η^6-C_6-PhzH)$Mo(PMe_3)_3$, (μ-η^6,η^6-PhzH)[$Mo(PMe_3)_3$]$_2$ and (η^4-C_4-PhzH)$_2Mo(PMe_3)_2$, each of which displays previously unknown coordination modes for phenazine. Both mononuclear (η^6-C_6-PhzH)$Mo(PMe_3)_3$ and dinuclear (μ-η^6,η^6-PhzH)[$Mo(PMe_3)_3$]$_2$ react with H_2 at room temperature to give the respective dihydride complexes, (η^4-C_4-PhzH)$Mo(PMe_3)_3H_2$ and (μ-η^6,η^4-PhzH)[$Mo(PMe_3)_3$][$Mo(PMe_3)_3H_2$]. A comparison of (η^6-C_6-PhzH)$Mo(PMe_3)_3$ with the anthracene (AnH) and acridine (AcrH) counterparts, (η^6-AnH)$Mo(PMe_3)_3$ and (η^6-C_6-AcrH)$Mo(PMe_3)_3$, indicates that oxidative addition of H_2 is promoted by incorporation of nitrogen substituents into the central ring. Furthermore, comparison of (η^6-C_6-PhzH)$Mo(PMe_3)_3$ with the quinoxaline (QoxH) analogue, (η^6-C_6-QoxH)$Mo(PMe_3)_3$, indicates that ring fusion also promotes oxidative addition of H_2. The mononitrogen quinoline (QH) and acridine compounds, (η^6-C_6-QH)$Mo(PMe_3)_3$ and (η^6-C_6-AcrH)$Mo(PMe_3)_3$, which respectively possess two and three fused six-membered rings, exhibit a similar trend, with the former being inert towards H_2, while the latter reacts rapidly to yield (η^4-C_4-AcrH)$Mo(PMe_3)_3H_2$. Ring fusion also promotes hydrogenation of the heterocyclic ligand, with (η^6-C_6-AcrH)$Mo(PMe_3)_3$ releasing 9,10-dihydroacridine upon treatment with H_2 in benzene at 95 °C. Furthermore, catalytic hydrogenation of acridine to a mixture of 9,10-dihydroacridine and 1,2,3,4-tetrahydroacridine may be achieved by treatment of (η^6-C_6-AcrH)$Mo(PMe_3)_3$ with acridine and H_2 at 95 °C.

Introduction

Hydrodenitrogenation (HDN), the means by which nitrogen is removed from compounds in fossil fuels, is a complex process that involves a variety of chemical sequences.[1−3] In order to procure a more detailed understanding of the reactions involved in HDN, we are actively developing the coordination chemistry of molybdenum (a key component of HDN catalysts) with heterocyclic aromatic nitrogen compounds.[4] Herein, we report the synthesis and structural characterization of phenazine (PhzH) complexes of molybdenum, thereby demonstrating that phenazine may adopt a variety of unprecedented coordination modes to this metal. In addition, we also describe how ring fusion impacts the reactivity of heterocyclic aromatic nitrogen compounds of the type (η^6-NHetH)$Mo(PMe_3)_3$ towards oxidative addition of H_2 and subsequent hydrogenation of the heterocycle.

Results and Discussion

Synthesis and Structural Characterization of Molybdenum Phenazine Complexes. Recent studies have demonstrated that polynuclear aromatic compounds inhibit both hydrodenitrogenation and hydrodesulfurization.[5] For this reason, it is particularly pertinent to investigate the means by which these compounds interact with molybdenum. In this regard, we have previously demonstrated that anthracene (AnH) and acridine (AcrH) react with $Mo(PMe_3)_6$ to give (η^6-AnH)$Mo(PMe_3)_3$[6] and (η^6-C_6-AcrH)$Mo(PMe_3)_3$,[4a] respectively, in which the aromatic ligands coordinate in an η^6 manner *via* one of the outer rings. We now report that the corresponding reaction of phenazine, a related trinuclear heterocycle (Figure 1), is considerably more complex and results in compounds that exhibit a variety of coordination modes.

Specifically, in addition to forming (η^6-C_6-PhzH)$Mo(PMe_3)_3$, $Mo(PMe_3)_6$ reacts with phenazine to yield (i) (η^4-C_4-PhzH)$_2$-$Mo(PMe_3)_2$, in which two phenazine ligands coordinate *via* η^4-

(1) Furimsky, E.; Massoth, F. E. *Catal. Rev.* **2005**, *47*, 297–489.
(2) Sanchez-Delgado, R. A. *Organometallic Modeling of the Hydrodesulfurization and Hydrodenitrogenation Reactions*; Kluwer Academic Publishers: Boston, 2002.
(3) (a) Angelici, R. J. *Polyhedron* **1997**, *16*, 3073–3088. (b) Weller, K. J.; Fox, P. A.; Gray, S. D.; Wigley, D. E. *Polyhedron* **1997**, *16*, 3139–3163. (c) Bianchini, C.; Meli, A.; Vizza, F. *Eur. J. Inorg. Chem.* **2001**, 43–68. (d) Borowski, A. F. *Pol. J. Chem.* **2006**, *80*, 205–226. (e) Sánchez-Delgado, R. A. *Comprehensive Organometallic Chemistry III*; Crabtree, R. H., Mingos, D. M. P., Eds.; Elsevier: Oxford, 2006; Vol. 1, Chapter 27. (f) Laine, R. M. *Catal. Rev.−Sci. Eng.* **1983**, *25*, 459–474.
(4) (a) Zhu, G.; Tanski, J. M.; Churchill, D. G.; Janak, K. E.; Parkin, G. *J. Am. Chem. Soc.* **2002**, *124*, 13658–13659. (b) Zhu, G.; Tanski, J. M.; Parkin, G. *Polyhedron* **2003**, *22*, 199–203. (c) Zhu, G.; Pang, K.; Parkin, G. *J. Am. Chem. Soc.* **2008**, *130*, 1564–1565. (d) Zhu, G.; Pang, K.; Parkin, G. *Inorg. Chim. Acta* **2008**, *361*, 3221–3229.
(5) (a) Choudhary, T. V.; Parrott, S.; Johnson, B. *Catal. Commun.* **2008**, *9*, 1853–1857. (b) Choudhary, T. V.; Parrott, S.; Johnson, B. *Environ. Sci. Technol.* **2008**, *42*, 1944–1947.
(6) Zhu, G.; Janak, K. E.; Figueroa, J. S.; Parkin, G. *J. Am. Chem. Soc.* **2006**, *128*, 5452–5461.

10.1021/ja901896x CCC: $40.75

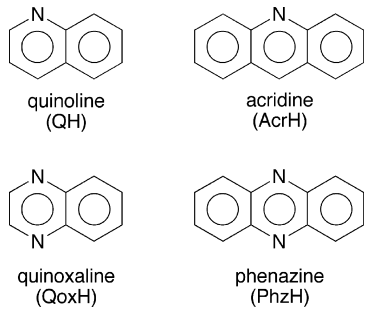

Figure 1. Binuclear and trinuclear aromatic nitrogen compounds.

Scheme 1

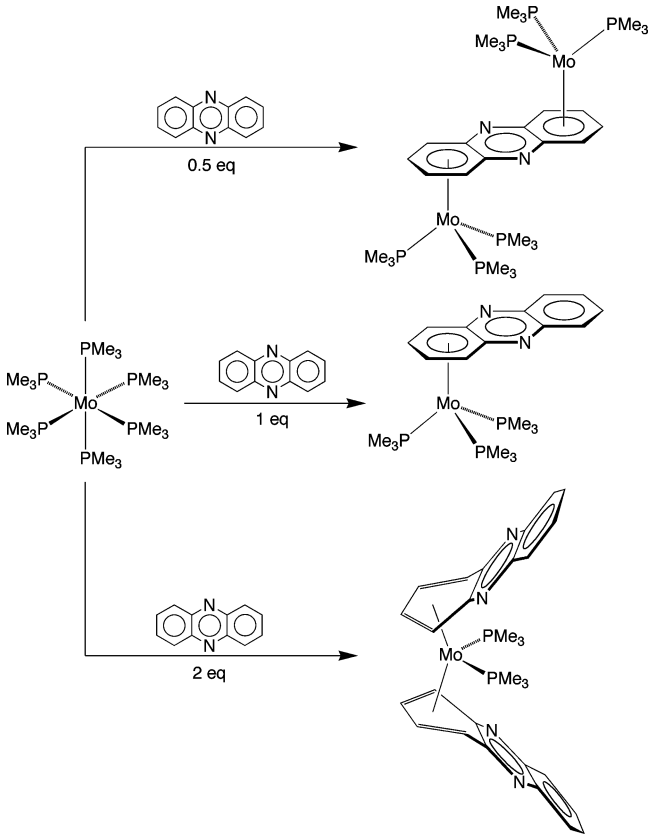

coordination modes, and (ii) (μ-η^6,η^6-PhzH)[Mo(PMe$_3$)$_3$]$_2$, a dinuclear compound in which the phenazine ligand bridges two metal centers[7] (Scheme 1). Thus, rather than only forming a complex in which phenazine coordinates to molybdenum in a 1:1 ratio, complexes with 1:2 and 2:1 stoichiometries have also been isolated.

The molecular structures of (η^6-C_6-PhzH)Mo(PMe$_3$)$_3$, (μ-η^6,η^6-PhzH)[Mo(PMe$_3$)$_3$]$_2$, and (η^4-C_4-PhzH)$_2$Mo(PMe$_3$)$_2$ have been determined by X-ray diffraction (Figures 2−4) and illustrate several interesting features. Of particular note, the phenazine ligand in each compound coordinates by using *only the carbon atoms* of the carbocyclic rings, a previously unknown coordination mode for phenazine. Specifically, in all other structurally characterized phenazine complexes, the ligand coordinates *via* its nitrogen atoms which, in many cases, are the *only* binding functionalities.[8,9] Another important feature of these compounds (discussed in more detail below) is that the phenazine ligands of (η^6-C_6-PhzH)Mo(PMe$_3$)$_3$ and (μ-η^6,η^6-PhzH)[Mo(PMe$_3$)$_3$]$_2$ adopt an η^6-coordination mode, while those in (η^4-C_4-PhzH)$_2$Mo(PMe$_3$)$_2$ adopt η^4-coordination modes such

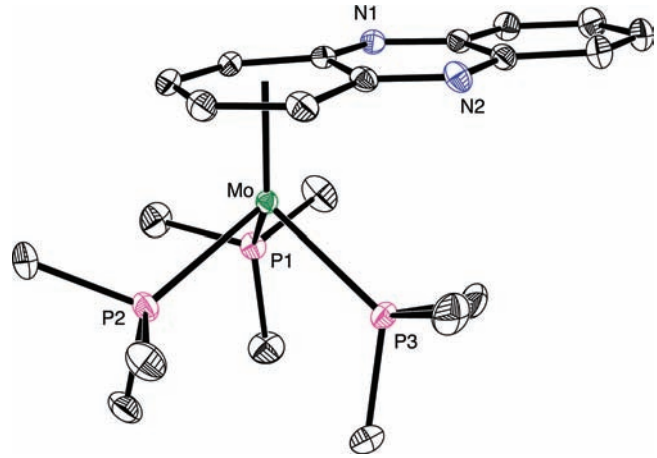

Figure 2. Molecular structure of (η^6-C_6-PhzH)Mo(PMe$_3$)$_3$.

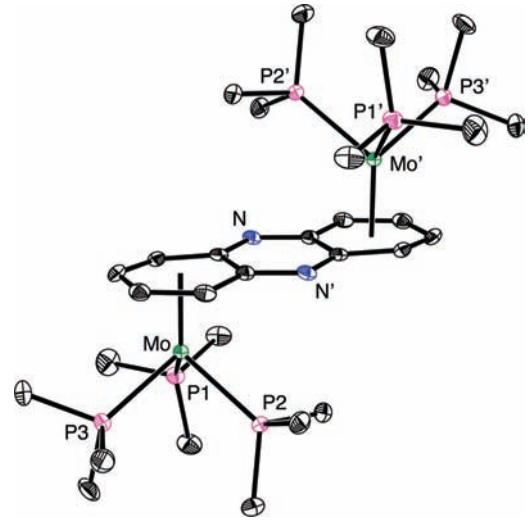

Figure 3. Molecular structure of (μ-η^6,η^6-PhzH)[Mo(PMe$_3$)$_3$]$_2$.

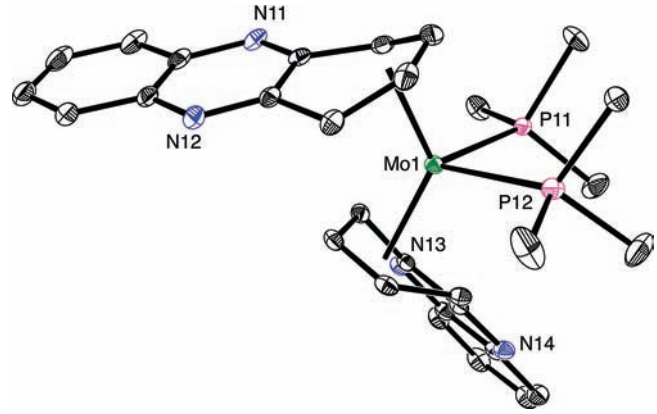

Figure 4. Molecular structure of (η^4-C_4-PhzH)$_2$Mo(PMe$_3$)$_2$ (only one of the two crystallographically independent molecules is shown).

that the compound is closely analogous to the butadiene complex (η^4-C$_4$H$_6$)$_2$Mo(PMe$_3$)$_2$.[10]

While the phenazine, acridine and anthracene complexes (η^6-C_6-PhzH)Mo(PMe$_3$)$_3$, (η^6-C_6-AcrH)Mo(PMe$_3$)$_3$[4a] and (η^6-AnH)Mo(PMe$_3$)$_3$,[6] are structurally analogous, each exhibiting coordination *via* a terminal carbocyclic ring, the facility with which these complexes are obtained differs considerably. Thus, whereas the reaction of Mo(PMe$_3$)$_6$ with anthracene requires

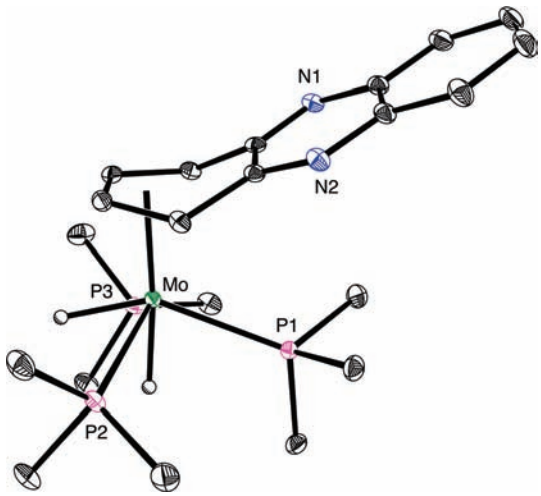

Figure 5. Molecular structure of (η^4-C_4-PhzH)Mo(PMe_3)$_3H_2$.

several days at 140 °C,[6] the corresponding reactions of acridine and phenazine require less than 1 day at 80 °C. It is, therefore, evident that the presence of nitrogen atoms in the central ring significantly promotes the reaction of the aromatic compound with Mo(PMe_3)$_6$, even though coordination of nitrogen is not observed in the final product. Although the mechanisms for the formation of these compounds are unknown, it is possible that the nitrogen atom assists the initial coordination of acridine and phenazine to the metal center through the κ^1-*N* mode, thereby facilitating a subsequent transformation to the η^6-coordinate species.

Oxidative Addition of H_2 to (η^6-NHetH)Mo(PMe_3)$_3$. Hydrogenation of the heterocyclic ring of polynuclear aromatic nitrogen compounds is considered to be an essential step that occurs prior to cleavage of the C−N bond during HDN.[3,11] For this reason, we have examined the reactivity of the above phenazine complexes towards H_2. In this regard, while the *bis*(phenazine) complex (η^4-C_4-PhzH)$_2$Mo(PMe_3)$_2$ does not react with H_2 at room temperature, (η^6-C_6-PhzH)Mo(PMe_3)$_3$ reacts instantaneously to give (η^4-C_4-PhzH)Mo(PMe_3)$_3H_2$ (Scheme 2).

Scheme 2

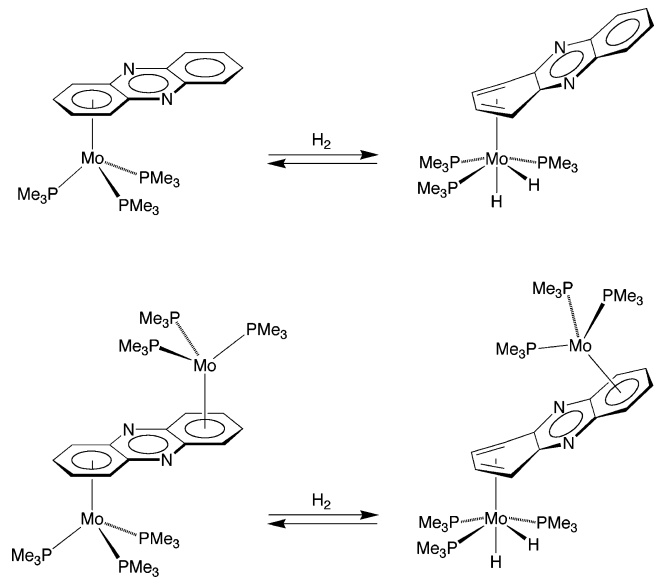

The molecular structure of (η^4-C_4-PhzH)Mo(PMe_3)$_3H_2$ has been determined by X-ray diffraction (Figure 5), which illustrates that the molecule has approximate C_s symmetry in which the mirror plane of the η^4-phenazine ligand is coincident with the plane comprising Mo, P1 and the two hydride ligands.[12] However, NMR spectroscopic studies indicate that, in solution at low temperature, the molecule possesses two configurations that differ according to the orientation of the η^4-phenazine ligand relative to that of the [Mo(PMe_3)$_3H_2$] moiety. Specifically, whereas one configuration has a structure in which the mirror plane of the η^4-phenazine ligand is coincident with the plane comprising Mo, P1 and the two hydride ligands,[12] i.e. that of the solid-state structure (Figure 5), the other configuration has a structure in which these planes are orthogonal to each other. Support for this proposal is provided by the structural characterization of other (η^4-NHetH)Mo(PMe_3)$_3H_2$ compounds described in more detail below.

The dinuclear complex (μ-η^6,η^6-PhzH)[Mo(PMe_3)$_3$]$_2$ is likewise subject to oxidative addition of H_2, but the reaction occurs selectively with only *one* of the molybdenum centers to give (μ-η^6,η^4-PhzH)[Mo(PMe_3)$_3$][Mo(PMe_3)$_3H_2$] (Scheme 2). X-ray diffraction indicates that the coordination geometries of the two metal centers of (μ-η^6,η^4-PhzH)[Mo(PMe_3)$_3$][Mo(PMe_3)$_3H_2$] (Figure 6) are similar to the respective geometries of mononuclear (η^6-C_6-PhzH)Mo(PMe_3)$_3$ and (η^4-C_4-PhzH)Mo(PMe_3)$_3$-H_2.

Interestingly, while the molybdenum coordination environments of mononuclear (η^6-C_6-PhzH)Mo(PMe_3)$_3$ and dinuclear

(7) For other dinuclear complexes that feature bridging fused polycyclic aromatic ligands, see: Ceccon, A.; Santi, S.; Orian, L.; Bisello, A. *Coord. Chem. Rev.* **2004**, *248*, 683–724.

(8) (a) Althoff, A.; Jutzi, P.; Lenze, N.; Neumann, B.; Stammler, A.; Stammler, H. G. *Organometallics* **2002**, *21*, 3018–3022. (b) Miyasaka, H.; Clérac, R.; Campos-Fernández, C. S.; Dunbar, K. R. *J. Chem. Soc., Dalton Trans.* **2001**, 858–861. (c) Whiteford, J. A.; Stang, P. J.; Huang, S. D. *Inorg. Chem.* **1998**, *37*, 5595–5601. (d) Munakata, M.; Kurodasowa, T.; Maekawa, M.; Honda, A.; Kitagawa, S. *J. Chem. Soc., Dalton Trans.* **1994**, 2771–2775. (e) Cotton, F. A.; Felthouse, T. R. *Inorg. Chem.* **1981**, *20*, 600–608. (f) Chesnut, D. J.; Plewak, D.; Zubieta, J. *J. Chem. Soc., Dalton Trans.* **2001**, 2567–2580. (g) Batten, S. R.; Hoskins, B. F.; Robson, R. *New J. Chem.* **1998**, *22*, 173–175. (h) Kurodasowa, T.; Munakata, M.; Matsuda, H.; Akiyama, S.; Maekawa, M. *J. Chem. Soc., Dalton Trans.* **1995**, 2201–2208. (i) Cotton, F. A.; Kim, Y. M.; Ren, T. *Inorg. Chem.* **1992**, *31*, 2723–2726.

(9) Dinuclear complexes with bridging η^3,η^3-coordination modes are also known. See, for example: (a) Evans, W. J.; Perotti, J. M.; Kozimor, S. A.; Champagne, T. M.; Davis, B. L.; Nyce, G. W.; Fujimoto, C. H.; Clark, R. D.; Johnston, M. A.; Ziller, J. W. *Organometallics* **2005**, *24*, 3916–3931. (b) Evans, W. J.; Gonzales, S. L.; Ziller, J. W. *J. Am. Chem. Soc.* **1994**, *116*, 2600–2608. (c) Scholz, J.; Scholz, A.; Weimann, R.; Janiak, C.; Schumann, H. *Angew. Chem., Int. Ed. Engl.* **1994**, *33*, 1171–1174.

(10) Brookhart, M.; Cox, K.; Cloke, F. G. N.; Green, J. C.; Green, M. L. H.; Hare, P. M.; Bashkin, J.; Derome, A. E.; Grebenik, P. D. *J. Chem. Soc., Dalton Trans.* **1985**, 423–433.

(11) However, it should be noted that there are examples of pyridine C−N bond cleavage, without prior hydrogenation, by metals other than molybdenum. See, for example: (a) Kleckley, T. S.; Bennett, J. L.; Wolczanski, P. T.; Lobkovsky, E. *J. Am. Chem. Soc.* **1997**, *119*, 247–248. (b) Gray, S. D.; Weller, K. J.; Bruck, M. A.; Briggs, P. M.; Wigley, D. E. *J. Am. Chem. Soc.* **1995**, *117*, 10678–10693. (c) Weller, K. J.; Filippov, I.; Briggs, P. M.; Wigley, D. E. *Organometallics* **1998**, *17*, 322–329. (d) Bailey, B. C.; Fan, H.; Huffman, J. C.; Baik, M.-H.; Mindiola, D. J. *J. Am. Chem. Soc.* **2006**, *128*, 6798–6799.

(12) The hydride ligands, which are in chemically reasonable positions, were located by X-ray diffraction, and their positions were refined. Furthermore, their locations are supported by DFT geometry optimization calculations.

(13) Zhu, G.; Janak, K. E.; Parkin, G. *Chem. Commun.* **2006**, 2501–2503.

(14) See, for example: Cotton, F. A.; Felthouse, T. R. *Inorg. Chem.* **1981**, *20*, 600–608.

Scheme 3

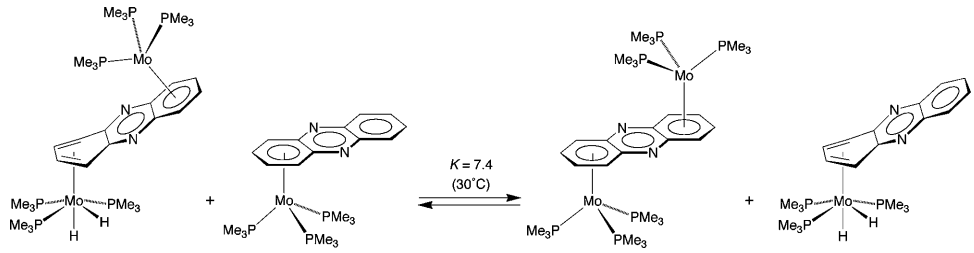

(μ-η^6,η^6-PhzH)[Mo(PMe$_3$)$_3$]$_2$ are similar, it is evident that coordination of the second molybdenum center does, nevertheless, exert an influence on the ability of the other molybdenum center to undergo oxidative addition of H_2. For example, dinuclear (μ-η^6,η^4-PhzH)[Mo(PMe$_3$)$_3$][Mo(PMe$_3$)$_3$H$_2$] transfers H_2 to (η^6-C_6-PhzH)Mo(PMe$_3$)$_3$, giving (μ-η^6,η^6-PhzH)[Mo(PMe$_3$)$_3$]$_2$ and (η^4-C_4-PhzH)Mo(PMe$_3$)$_3$H$_2$ with $K = 7.4$ at 30 °C (Scheme 3), thereby demonstrating that coordination of the second molybdenum center inhibits oxidative addition of H_2.

Influence of Nitrogen Atom Substituents on Oxidative Addition of H_2. Comparison of the reactivity of the phenazine, acridine and anthracene complexes (η^6-C_6-PhzH)Mo(PMe$_3$)$_3$, (η^6-C_6-AcrH)Mo(PMe$_3$)$_3$ and (η^6-AnH)Mo(PMe$_3$)$_3$, provides a means to identify how nitrogen atom substituents in an adjacent fused ring influence the ability of the metal center to undergo oxidative addition of H_2. In this regard, we have previously reported that (η^6-AnH)Mo(PMe$_3$)$_3$ reacts reversibly with H_2 at room temperature to give (η^4-AnH)Mo(PMe$_3$)$_3$H$_2$.[6,13] It is, therefore, not surprising that the acridine counterpart (η^6-C_6-AcrH)Mo(PMe$_3$)$_3$[4a] also reacts rapidly with H_2 at room temperature to yield (η^4-C_4-AcrH)Mo(PMe$_3$)$_3$H$_2$ (Scheme 4). The molecular structure of (η^4-C_4-AcrH)Mo(PMe$_3$)$_3$H$_2$ has been determined by X-ray diffraction, as illustrated in Figure 7. Significantly, (η^4-C_4-AcrH)Mo(PMe$_3$)$_3$H$_2$ is the first structurally characterized complex that exhibits an η^4-coordination mode for acridine, which otherwise typically coordinates in a κ^1-N manner.[14,15] Also of note, the structure of (η^4-C_4-AcrH)Mo(PMe$_3$)$_3$-H$_2$ differs from that of (η^4-C_4-PhzH)Mo(PMe$_3$)$_3$H$_2$ by virtue of the fact that the long axis of the η^4-acridine ligand does not lie in the mirror plane of the [Mo(PMe$_3$)$_3$H$_2$] moiety. The solid-state structure of (η^4-C_4-AcrH)Mo(PMe$_3$)$_3$H$_2$ is, nevertheless, in accord with that proposed for one of the configurations of (η^4-C_4-PhzH)Mo(PMe$_3$)$_3$H$_2$ observed in solution at low temperature (see above). Furthermore, the anthracene complex

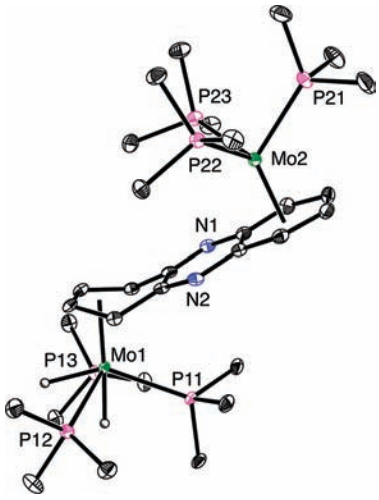

Figure 6. Molecular structure of (μ-η^6,η^4-PhzH)[Mo(PMe$_3$)$_3$][Mo(PMe$_3$)$_3$-H$_2$].

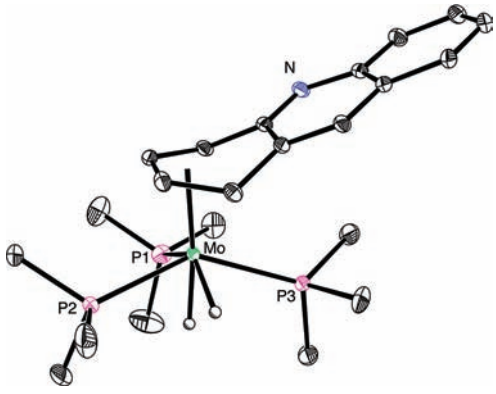

Figure 7. Molecular structure of (η^4-C_4-AcrH)Mo(PMe$_3$)$_3$H$_2$.

Scheme 4

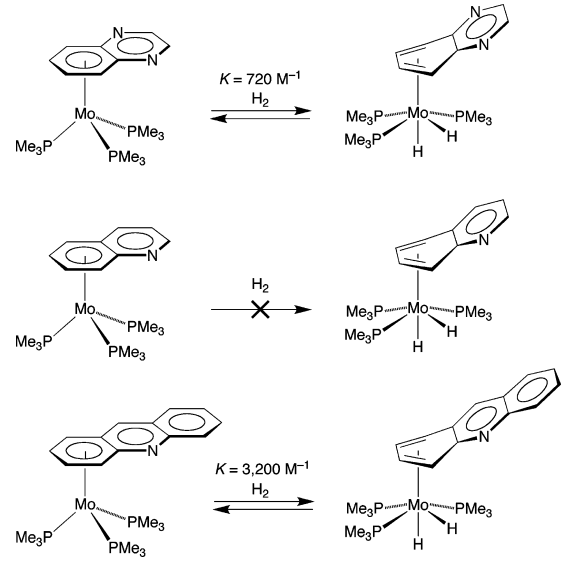

Table 1. Equilibrium Constant Data for Oxidative Addition of H_2 to (η^6-ArH)Mo(PMe$_3$)$_3$ in C_6D_6 at 30 °C

	K /M^{-1}
(η^6-AnH)Mo(PMe$_3$)$_3$[a]	1.6×10^4
(η^6-C_6-AcrH)Mo(PMe$_3$)$_3$[b]	3.2×10^4
(η^6-C_6-PhzH)Mo(PMe$_3$)$_3$[b]	5.8×10^6
(μ-η^6,η^6-PhzH)[Mo(PMe$_3$)$_3$]$_2$[b]	7.8×10^5
(η^6-C_6-QoxH)Mo(PMe$_3$)$_3$[c]	7.2×10^2

[a] Data taken from ref 13. [b] Value determined from a thermodynamic cycle which couples experimentally measured values for H_2 exchange between the various metal centers (Schemes 3 and 4) with the oxidative addition of H_2 to (η^6-AnH)Mo(PMe$_3$)$_3$. [c] Value at room temperature.

Scheme 5

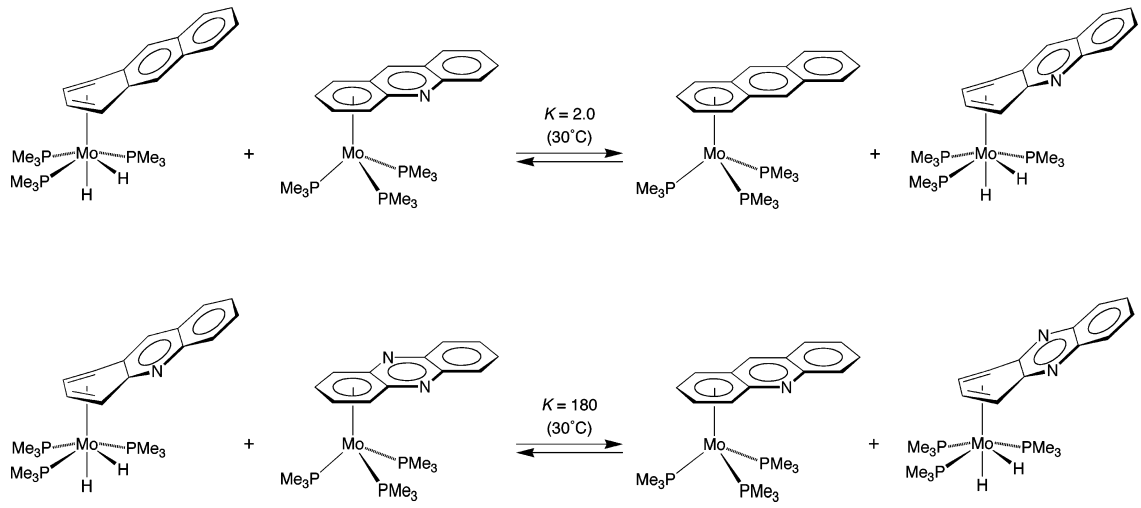

(η^4-AnH)Mo(PMe_3)$_3H_2$ (Figure 8) exhibits the same configuration as that of (η^4-AcrH)Mo(PMe_3)$_3H_2$ in the solid state.

As with (η^6-AnH)Mo(PMe_3)$_3$,[6,13] the oxidative addition of H_2 to (η^6-C_6-AcrH)Mo(PMe_3)$_3$ and (η^6-C_6-PhzH)Mo(PMe_3)$_3$ is reversible and a series of H_2 transfer experiments demonstrates that the equilibrium constant for oxidative addition increases in the sequence $K_{AnH} < K_{AcrH} < K_{PhzH}$ (Table 1). Specifically, (η^4-AnH)Mo(PMe_3)$_3H_2$ transfers H_2 to (η^6-C_6-AcrH)Mo(PMe_3)$_3$ giving (η^4-C_4-AcrH)Mo(PMe_3)$_3H_2$ ($K = 2.0$ at 30 °C), while (η^4-C_4-AcrH)Mo(PMe_3)$_3H_2$ transfers H_2 to (η^6-C_6-PhzH)-Mo(PMe_3)$_3$ giving (η^4-C_4-PhzH)Mo(PMe_3)$_3H_2$ ($K = 1.8 \times 10^2$ at 30 °C), as illustrated in Scheme 5. It is, therefore, evident that the presence of nitrogen atoms in the central ring increases the ability of the metal center to undergo oxidative addition of H_2. In support of these observations, density functional theory (DFT) calculations also predict that the exothermicity for oxidative addition of H_2 increases with the number of nitrogen atoms in the central ring (Table 2).

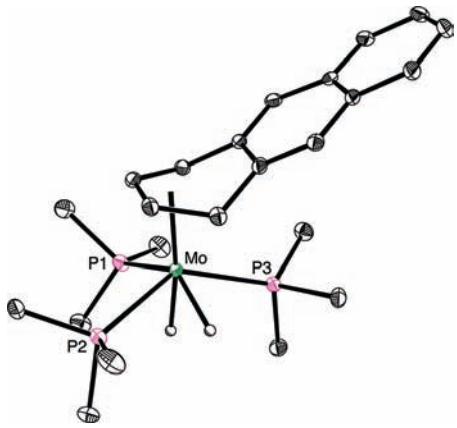

Figure 8. Molecular structure of (η^4-AnH)Mo(PMe_3)$_3H_2$.

Influence of Ring Fusion on Oxidative Addition of H_2. Our previous experimental and computational studies concerned with the benzene, naphthalene and anthracene compounds, (η^6-PhH)-Mo(PMe_3)$_3$, (η^6-NpH)Mo(PMe_3)$_3$ and (η^6-AnH)Mo(PMe_3)$_3$, respectively, have demonstrated that ring fusion promotes oxidative addition of H_2.[6] In particular, the dihydride only becomes experimentally observable for the anthracene system. We have now extended this study to include heterocyclic aromatic compounds.

Comparison of the reactivity of related mononitrogen heterocyclic systems, namely the quinoline (QH) and acridine derivatives, which respectively possess two and three fused six-membered rings, demonstrates that ring fusion promotes oxidative addition in this system. Thus, whereas (η^6-C_6-AcrH)Mo-(PMe_3)$_3$ reacts with H_2 to give (η^4-C_4-AcrH)Mo(PMe_3)$_3H_2$ (Scheme 4), (η^6-C_6-QH)Mo(PMe_3)$_3$ is inert towards H_2 under comparable conditions.[4a]

Table 2. Computational ΔH^{SCF} for Oxidative Addition of H_2 to (η^6-NHetH)Mo(PH_3)$_3$ Giving Two Isomers of (η^4-NHetH)Mo(PH_3)$_3H_2$[a]

	symmetric (η^4-NHetH)Mo(PH_3)$_3H_2$	asymmetric (η^4-NHetH)Mo(PH_3)$_3H_2$
(η^6-AnH)Mo(PH_3)$_3$	−1.77	−4.19
(η^6-C_6-AcrH)Mo(PH_3)$_3$	−3.30	−5.67
(η^6-C_6-PhzH)Mo(PH_3)$_3$	−6.43	−8.04

[a] Values in kcal mol^{-1}.

A similar effect is observed upon comparison of the quinoxaline (QoxH) and phenazine compounds, (η^6-C_6-QoxH)-Mo(PMe_3)$_3$[4c] and (η^6-C_6-PhzH)Mo(PMe_3)$_3$, both of which feature two nitrogen atoms in the adjacent fused ring. Thus, in contrast to the rapid reaction of (η^6-C_6-PhzH)Mo(PMe_3)$_3$ with H_2 to give (η^4-C_4-PhzH)Mo(PMe_3)$_3H_2$, the quinoxaline counterpart (η^6-C_6-QoxH)Mo(PMe_3)$_3$,[4c] with only two fused six-membered rings, requires several days to react and yields (η^4-C_4-QoxH)Mo(PMe_3)$_3H_2$ (Scheme 4) as only a component of an equilibrium mixture under 1 atm of H_2 ($K = 7.2 \times 10^2$ M^{-1} at room temperature). As such, it demonstrates that, in this system, ring-fusion increases the reactivity of the metal center towards oxidative addition of H_2 by a factor of $\sim 10^4$ in equilibrium constant, an observation that may be viewed as a heterocyclic analogue of the "anthracene effect".[6]

Despite the fact that (η^4-C_4-QoxH)Mo(PMe_3)$_3H_2$ is only observed as a component of an equilibrium mixture, the compound has been structurally characterized by X-ray diffraction. Most interestingly, the asymmetric unit consists of two molecules that differ by the orientation of the η^4-quinoxaline ligand relative to the [Mo(PMe_3)$_3H_2$] moiety (Figure 9). As such, it is evident that (η^4-C_4-QoxH)Mo(PMe_3)$_3H_2$ exhibits *both* of the configurations discussed above for the phenazine, acridine and anthracene compounds. In view of the fact that each of

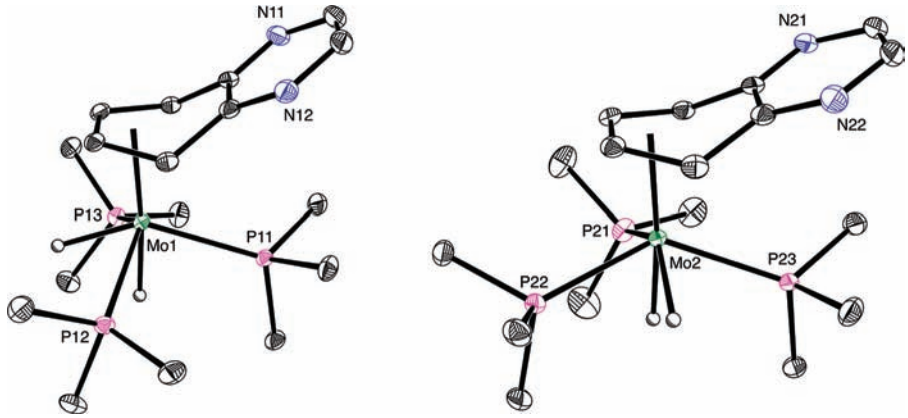

Figure 9. Molecular structures of the two conformations of (η^4-C_4-QoxH)Mo(PMe_3)$_3$$H_2$.

Scheme 6

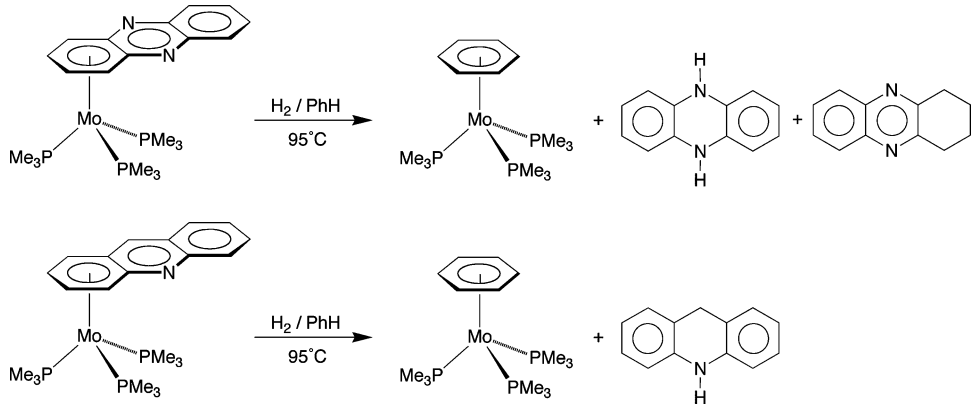

these compounds exhibits two conformations in solution, it is possible that the different solid-state structures may merely reflect crystal packing effects.

The ability to spectroscopically observe and structurally characterize (η^4-C_4-QoxH)Mo(PMe_3)$_3$$H_2$ is also noteworthy because the corresponding species were not observed for the quinoline and naphthalene derivatives. As such, it provides a further illustration that nitrogen substituents in an adjacent fused ring promote oxidative addition of H_2.

While (η^6-C_6-PhzH)Mo(PMe_3)$_3$ and (η^6-C_6-AcrH)Mo(PMe_3)$_3$ only undergo oxidative addition of H_2 at room temperature, the phenazine and acridine ligands are hydrogenated at elevated temperatures. Thus, (η^6-C_6-PhzH)Mo(PMe_3)$_3$ releases a mixture of 5,10-dihydrophenazine and 1,2,3,4-tetrahydrophenazine upon treatment with H_2 in benzene at 95 °C,[16] while (η^6-C_6-AcrH)Mo(PMe_3)$_3$ releases 9,10-dihydroacridine under the same conditions; in each case, the principal molybdenum-containing product is (η^6-PhH)Mo(PMe_3)$_3$ (Scheme 6).

In contrast to the hydrogenation of acridine, the quinoline counterpart (η^6-C_6-QH)Mo(PMe_3)$_3$ is stable under these conditions,[4a] from which it is evident that ring fusion also promotes hydrogenation of the heterocyclic ligand. Furthermore, although the turnover number is low (7.2 turnovers over a period of 21 days), acridine is catalytically hydrogenated in the presence of (η^6-C_6-AcrH)Mo(PMe_3)$_3$ and H_2 at 95 °C. Under these conditions, the principal products are a 2:3 mixture of 9,10-dihydroacridine and 1,2,3,4-tetrahydroacridine.[17] The formation of 1,2,3,4-tetrahydroacridine is noteworthy because several studies indicate that acridine is typically selectively hydrogenated at the central heterocyclic ring to give 9,10-dihydroacridine.[18] In fact, we are aware of only one catalyst that selectively hydrogenates the carbocyclic rings of acridine, namely RuH_2(η^2-H_2)$_2$(PCy_3)$_2$, as reported by Borowski and Sabo-Etienne.[15]

Structural Comparison of η^4 and η^6-Phenazine Complexes. The phenazine complexes discussed above belong to two classes according to whether the ligand binds in an η^6 or η^4 manner *via* the carbon atoms, both of which are distinct from the

(15) The η^4-acridine complex (η^4-AcrH)RuH_2(PCy_3)$_2$ has been spectroscopically characterized. See: Borowski, A. F.; Sabo-Etienne, S.; Donnadieu, B.; Chaudret, B. *Organometallics* **2003**, *22*, 1630–1637.

(16) In this regard the hydrogenation of phenazine to 5,10-dihydrophenazine and 1,2,3,4-tetrahydrophenazine has been proposed to occur prior to hydrodenitrogenation. See: Nagai, M.; Sawahiraki, K.; Kabe, T. *Nippon Kagaku Kaishi* **1982**, *1*, 115–119.

(17) Catalytic hydrogenation of acridine by $Rh(PPh_3)_3Cl$ yields a similar mixture of 1,2,3,4-tetrahydroacridine and 9,10-dihydroacridine to that observed here. See: Fish, R. H.; Tan, J. L.; Thormodsen, A. D. *J. Org. Chem.* **1984**, *49*, 4500–4505.

(18) For examples of hydrogenation of acridine to 9,10-dihydroacridine, see: (a) Rosales, M.; Castillo, S.; González, A.; González, L.; Molina, K.; Navarro, J.; Pacheco, I.; Perez, H. *Transition Met. Chem.* **2004**, *29*, 221–228. (b) Fish, R. H.; Baralt, E.; Smith, S. J. *Organometallics* **1991**, *10*, 54–56. (c) Fish, R. H.; Thormodsen, A. D.; Cremer, G. A. *J. Am. Chem. Soc.* **1982**, *104*, 5234–5237. (d) Lee, C.; Steele, B. R.; Sutherland, R. G. *J. Organomet. Chem.* **1980**, *186*, 265–270. (e) Baralt, E.; Smith, S. J.; Hurwitz, J.; Horváth, I. T.; Fish, R. H. *J. Am. Chem. Soc.* **1992**, *114*, 5187–5196. (f) Fish, R. H. *Ann. N.Y. Acad. Sci.* **1983**, *415*, 292–301. (g) Chin, C. S.; Park, Y.; Lee, B. *Catal. Lett.* **1995**, *31*, 239–243. (h) Rosales, M.; Navarro, J.; Sánchez, L.; González, A.; Alvarado, Y.; Rubio, R.; De La Cruz, C.; Rajmankina, T. *Transition Met. Chem.* **1996**, *21*, 11–15. (i) Rosales, M.; Vallejo, R.; Soto, J. J.; Chacón, G.; González, A.; González, B. *Catal. Lett.* **2006**, *106*, 101–105.

Table 3. Average Mo−C Bond Lengths for the Outer, Central and Ring Junction Carbon Atoms of [(η^6-ArH)Mo] Interactions As Determined by X-ray Diffraction

	d(Mo−C_{outer})/Å	d(Mo−$C_{central}$)/Å	d(Mo−$C_{junction}$)/Å	slip parameter/Å	hinge angle/deg
(η^6-C_6-PhzH)Mo(PMe_3)$_3$	2.282	2.302	2.407	0.125	4.7
(μ-η^6,η^6-PhzH)[Mo(PMe_3)$_3$]$_2$	2.290	2.292	2.406	0.116	5.4
(μ-η^6,η^4-PhzH)[Mo(PMe_3)$_3$][Mo(PMe_3)$_3H_2$]	2.288	2.280	2.347	0.059	4.1
(η^6-C_6-AcrH)Mo(PMe_3)$_3$[a]	2.288	2.271	2.393	0.105	5.8
(η^6-AnH)Mo(PMe_3)$_3$[b]	2.273	2.283	2.416	0.143	6.0
	2.278	2.288	2.421	0.143	5.8

[a] Data taken from ref 4a. [b] Data taken from ref 6 (values for two independent molecules).

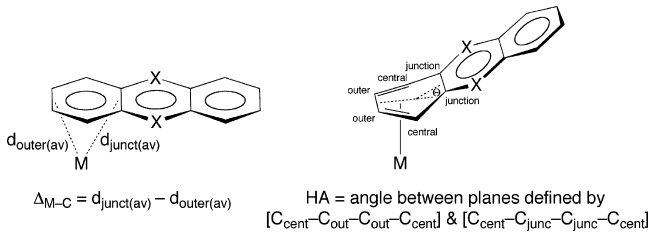

Figure 10. Definition of slip parameter (Δ_{M-C}) and hinge angle (HA).

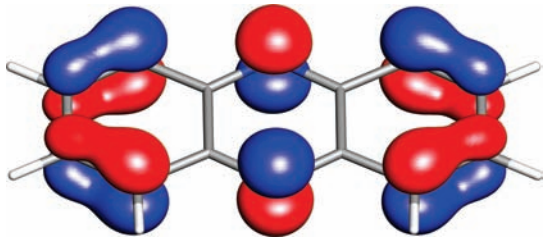

Figure 11. The highest occupied π molecular orbital of phenazine.

previously reported modes for phenazine that involve coordination *via* the nitrogen atoms.[8,9] Thus, (η^6-C_6-PhzH)Mo(PMe_3)$_3$ and (μ-η^6,η^6-PhzH)[Mo(PMe_3)$_3$]$_2$ exhibit η^6-coordination, while (η^4-C_4-PhzH)Mo(PMe_3)$_3H_2$ and (η^4-C_4-PhzH)$_2$Mo(PMe_3)$_2$ possess η^4-coordination modes, and (μ-η^6,η^4-PhzH)[Mo(PMe_3)$_3$][Mo(PMe_3)$_3H_2$] exhibits both modes.

Despite the fact that (η^6-C_6-PhzH)Mo(PMe_3)$_3$ and (μ-η^6,η^6-PhzH)[Mo(PMe_3)$_3$]$_2$ both exhibit η^6-coordination, the phenazine ligands do not coordinate symmetrically. For example, the Mo−C bond distances for the carbocyclic ring of (η^6-C_6-PhzH)Mo(PMe_3)$_3$ increase in the sequence Mo−$C_{outer(av)}$ [2.28 Å] < Mo−$C_{central(av)}$ [2.30 Å] < Mo−$C_{ring\ junction(av)}$ [2.41 Å] (Table 3). As such, the phenazine ligand slips so that the ring junction becomes more distant from the metal. The displacement of the heterocycle from symmetric η^6-coordination may be expressed in terms of a slip parameter (Δ_{M-C}), defined as the difference between (i) the average distance from the metal center to the two ring junction carbons and (ii) the average distance from the metal to the outer carbon atoms (Figure 10). In this regard, the slip parameters for (η^6-C_6-PhzH)Mo(PMe_3)$_3$ and (μ-η^6,η^6-PhzH)[Mo(PMe_3)$_3$]$_2$ are comparable to those of the acridine and anthracene complexes, (η^6-C_6-AcrH)Mo(PMe_3)$_3$ and (η^6-AnH)-Mo(PMe_3)$_3$, as summarized in Table 3. Similar slippages are also observed for η^6-complexes of other fused-ring aromatic systems.[19]

The origin of the slippage may be traced to the nature of the highest occupied π molecular orbital (π-HOMO) of phenazine (Figure 11). In this regard, the bonding in transition metal−(η^6-arene) compounds is generally considered to involve π-donation from the arene HOMO, supplemented by δ-backbonding to the arene LUMO,[20,21] Indeed, we recently rationalized the ring-slippage of the naphthalene and anthracene compounds, (η^6-NpH)Mo(PMe_3)$_3$ and (η^6-AnH)Mo(PMe_3)$_3$, in terms of this former interaction.[6] Specifically, the π-HOMO of a ring-fused arene is localized on the outer carbon atoms, which causes the arene to slip in order to maximize the π-interaction with the metal d orbital. The π-HOMO of phenazine is also largely localized on the outer carbon atoms (Figure 11), thereby providing an explanation of the slippage in (η^6-C_6-PhzH)-Mo(PMe_3)$_3$ and (μ-η^6,η^6-PhzH)[Mo(PMe_3)$_3$]$_2$.

In contrast to the flat nature of the η^6-phenazine ligands in (η^6-C_6-PhzH)Mo(PMe_3)$_3$ and (μ-η^6,η^6-PhzH)[Mo(PMe_3)$_3$]$_2$, the η^4-phenazine ligands of (η^4-C_4-PhzH)Mo(PMe_3)$_3H_2$ and (η^4-C_4-PhzH)$_2$Mo(PMe_3)$_2$ exhibit a distinct fold at the central carbon atoms of the coordinated ring. The folding of the phenazine ligand may be expressed in terms of the hinge angle (HA), defined as the dihedral angle between the planes comprising (i) the η^4-diene component and (ii) the central and junction carbon atoms of the coordinated ring (Figure 10). In this regard, the phenazine ligand of (η^4-C_4-PhzH)Mo(PMe_3)$_3H_2$ is folded by 34.5°, while the phenazine ligands of the two crystallographically independent molecules of (η^4-C_4-PhzH)$_2$Mo(PMe_3)$_2$ exhibit hinge angles in the range 28.4−37.3°. For comparison, the hinge angles of the η^6-phenazine complexes are only in the range 4.1−5.4°. In addition to the hinge angle, another indication of the folding is provided by the slip parameter, which increases from 0.13 Å for (η^6-C_6-PhzH)Mo(PMe_3)$_3$ to 0.91 Å for (η^4-C_4-PhzH)Mo(PMe_3)$_3H_2$ (Tables 3 and 4).

The folding observed in the η^4-phenazine complexes is also observed in the related anthracene,[22] acridine, and quinoxaline complexes (Figures 7−9). Furthermore, a common feature of each of these complexes is that the Mo−C bonds for the outer carbon atoms are shorter than those for the central carbon atoms (Table 4). While a simple explanation of the bending of the aromatic ligands is to preserve an 18-electron configuration of the metal center, a more complete analysis indicates that folding

(19) See, for example: (a) Chen, J.; Angelici, R. J. *Organometallics* **1999**, *18*, 5721–5724. (b) Vecchi, P. A.; Ellern, A.; Angelici, R. J. *Organometallics* **2005**, *24*, 3725–3730. (c) Rudd, J. A.; Angelici, R. J. *Inorg. Chim. Acta* **1995**, *240*, 393–398. (d) Hanic, F.; Mills, O. S. *J. Organomet. Chem.* **1968**, *11*, 151–158.

(20) Muetterties, E. L.; Bleeke, J. R.; Wucherer, E. J.; Albright, T. A. *Chem. Rev.* **1982**, *82*, 499–525.

(21) For calculations on (η^6-arene)ML_3 complexes, see: (a) Howell, J. A. S.; Ashford, N. F.; Dixon, D. T.; Kola, J. C.; Albright, T. A.; Kwang, S. K. *Organometallics* **1991**, *10*, 1852–1864. (b) Albright, T. A.; Hofmann, P.; Hoffmann, R.; Lillya, C. P.; Dobosh, P. A. *J. Am. Chem. Soc.* **1983**, *105*, 3396–3411. (c) Byers, B. P.; Hall, M. B. *Organometallics* **1987**, *6*, 2319–2325. (d) Rogers, R. D.; Atwood, J. L.; Albright, T. A.; Lee, W. A.; Rausch, M. D. *Organometallics* **1984**, *3*, 263–270. (e) Albright, T. A.; Hofmann, P.; Hoffmann, R. *J. Am. Chem. Soc.* **1977**, *99*, 7546–7557. (f) Albright, T. A.; Carpenter, B. K. *Inorg. Chem.* **1980**, *19*, 3092–3097. (g) Cohen, R.; Weitz, E.; Martin, J. M. L.; Ratner, M. A. *Organometallics* **2004**, *23*, 2315–2325. (h) Albright, T. A. *Acc. Chem. Res.* **1982**, *15*, 149–155. (i) Asirvatham, V. S.; Gruhn, N. E.; Lichtenberger, D. L.; Ashby, M. T. *Organometallics* **2000**, *19*, 2215–2227.

Table 4. Average Mo−C Bond Lengths for the Outer, Central and Ring Junction Carbon Atoms of [(η^4-ArH)Mo] Complexes As Determined by X-ray Diffraction

	d(Mo−C_{outer})/Å	d(Mo−$C_{central}$)/Å	d(Mo···$C_{junction}$)/Å	slip parameter/Å	hinge angle/deg
(η^4-C_4-PhzH)Mo(PMe_3)$_3H_2$	2.214	2.356	3.119	0.905	34.5
(μ-η^6,η^4-PhzH)[Mo(PMe_3)$_3$][Mo(PMe_3)$_3H_2$]	2.208	2.349	3.134	0.926	35.4
(η^4-C_4-AcrH)Mo(PMe_3)$_3H_2$	2.226	2.355	3.127	0.901	35.0
(η^4-AnH)Mo(PMe_3)$_3H_2$	2.251	2.352	3.167	0.916	39.2
(η^4-C_4-PhzH)$_2$Mo(PMe_3)$_2$ #1[a]	2.220	2.360	3.152	0.932	37.3
	2.288	2.390	3.029	0.741	28.4
(η^4-C_4-PhzH)$_2$Mo(PMe_3)$_2$ #2[a]	2.227	2.349	3.131	0.904	36.5
	2.296	2.358	3.045	0.749	33.1
(η^4-C_4-QoxH)Mo(PMe_3)$_3H_2$ (sym)[a]	2.216	2.337	3.152	0.936	39.3
(η^4-C_4-QoxH)Mo(PMe_3)$_3H_2$ (asym)[a]	2.251	2.355	3.098	0.847	35.1

[a] Two crystallographically independent molecules.

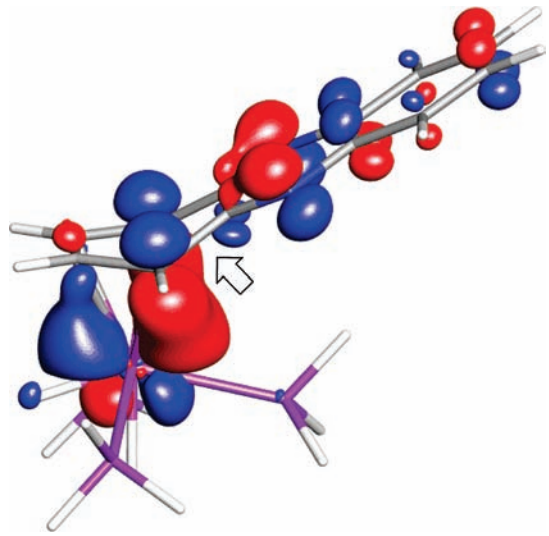

Figure 12. Occupied back-bonding molecular orbital of (η^4-C_4-PhzH)Mo(PH_3)$_3H_2$ for which the out-of-phase component with the d orbital (marked with an arrow) promotes folding of the heterocycle.

serves to stabilize the orbital involved in the metal-to-ligand backbonding interaction by minimizing the antibonding component between the metal and the two carbon atoms of the ring junction (Figure 12).[23]

Conclusions

In summary, phenazine reacts with Mo(PMe_3)$_6$ to give (η^6-C_6-PhzH)Mo(PMe_3)$_3$, (μ-η^6,η^6-PhzH)[Mo(PMe_3)$_3$]$_2$ and (η^4-C_4-PhzH)$_2$Mo(PMe_3)$_2$, in which the phenazine exhibits novel coordination modes *via* only the carbon atoms. Comparison of the reactivity of the phenazine, acridine and anthracene complexes respectively (η^6-C_6-PhzH)Mo(PMe_3)$_3$, (η^6-C_6-AcrH)Mo(PMe_3)$_3$ and (η^6-AnH)Mo(PMe_3)$_3$, demonstrates that incorporation of nitrogen substituents into the central ring promotes oxidative addition of H_2. The same conclusion is obtained by comparison of the reactivity of compounds that feature two fused rings, namely the quinoxaline and quinoline complexes, (η^6-C_6-QoxH)Mo(PMe_3)$_3$ and (η^6-C_6-QH)Mo(PMe_3)$_3$. Furthermore, comparison of the reactivity of (i) (η^6-C_6-PhzH)Mo(PMe_3)$_3$ and (η^6-C_6-QoxH)Mo(PMe_3)$_3$, and (ii) (η^6-C_6-AcrH)Mo(PMe_3)$_3$ and (η^6-C_6-QH)Mo(PMe_3)$_3$ demonstrates that ring fusion promotes oxidative addition of H_2.

Experimental Section

General Considerations. All manipulations were performed using a combination of glovebox, high vacuum, and Schlenk techniques under an argon atmosphere unless otherwise specified.[24] Solvents were purified and degassed by standard procedures. ^{1}H NMR spectra were measured on Bruker 300 DRX, Bruker 400 DRX, and Bruker Avance 500 DMX spectrometers. ^{1}H chemical shifts are reported in ppm relative to $SiMe_4$ ($\delta = 0$) and were referenced internally with respect to the protio solvent impurity (δ 7.16 for C_6D_6, 2.09 for C_7D_8, 1.38 for C_6D_{12}, and 7.26 for $CDCl_3$).[25,26] ^{13}C NMR spectra are reported in ppm relative to $SiMe_4$ ($\delta = 0$) and were referenced internally with respect to the solvent (δ 128.06 for C_6D_6).[25] ^{31}P chemical shifts are reported in ppm relative to 85% H_3PO_4 ($\delta = 0$) and were referenced using $P(OMe)_3$ ($\delta = 141.0$) as an external standard. Coupling constants are given in hertz. Infrared spectra were recorded on Nicolet Avatar 370 DTGS spectrometer and are reported in cm^{-1}. Mass spectra were obtained on a Micromass Quadrupole-Time-of-Flight mass spectrometer using fast atom bombardment (FAB). Mo(PMe_3)$_6$,[27] (η^6-AnH)Mo(PMe_3)$_3$,[6] (η^4-AnH)Mo(PMe_3)$_3H_2$,[6] (η^6-C_6-AcrH)Mo(PMe_3)$_3$,[4a] (η^6-C_6-QH)Mo(PMe_3)$_3$[4a] and (η^6-C_6-QoxH)Mo(PMe_3)$_3$[4c] were prepared by the literature methods.

X-ray Structure Determinations. X-ray diffraction data were collected on either a Bruker Apex II diffractometer or a Bruker P4 diffractometer equipped with a SMART CCD detector. Crystal data, data collection and refinement parameters are summarized in Table S1. The structures were solved using direct methods and standard

(22) For other examples of bent η^4-anthracene compounds, see: (a) Brennessel, W. W.; Ellis, J. E.; Pomije, M. K.; Sussman, V. J.; Urnezius, E.; Young, V. G., Jr. *J. Am. Chem. Soc.* **2002**, *124*, 10258–10259. (b) Brennessel, W. W.; Ellis, J. E.; Roush, S. N.; Strandberg, B. R.; Woisetschläger, O. E.; Young, V. G., Jr. *Chem. Commun.* **2002**, 2356–2357. (c) Jilek, R. E.; Jang, M.; Smolensky, E. D.; Britton, J. D.; Ellis, J. E. *Angew. Chem., Int. Ed.* **2008**, *47*, 8692–8695. (d) Sussman, V. J.; Ellis, J. E. *Angew. Chem., Int. Ed.* **2008**, *47*, 484–489. (e) Brennessel, W. W.; Jilek, R. E.; Ellis, J. E. *Angew. Chem., Int. Ed.* **2007**, *46*, 6132–6136. (f) Mashima, K.; Nakayama, Y.; Kaidzu, M.; Ikushima, N.; Nakamura, A. *J. Organomet. Chem.* **1998**, *557*, 3–12. (g) Müller, J.; Gaede, P. E.; Hirsch, C.; Qiao, K. *J. Organomet. Chem.* **1994**, *472*, 329–335. (h) Boese, R.; Stanger, A.; Stellberg, P.; Shazar, A. *Angew. Chem., Int. Ed. Engl.* **1993**, *32*, 1475–1477. (i) Protasiewicz, J. D.; Bianconi, P. A.; Williams, I. D.; Liu, S.; Rao, C. P.; Lippard, S. J. *Inorg. Chem.* **1992**, *31*, 4134–4142. (j) Bennett, M. A.; Bown, M.; Hockless, D. C. R. *Aust. J. Chem.* **2000**, *53*, 507–515.

(23) For a related example of folding to minimize this type of antibonding interaction in the anthracene compound, (η^6-AnH)Mo(PMe_3)$_3$, see ref 6.

(24) (a) McNally, J. P.; Leong, V. S.; Cooper, N. J. In *Experimental Organometallic Chemistry*; Wayda, A. L., Darensbourg, M. Y., Eds.; American Chemical Society: Washington, DC, 1987; Chapter 2, pp 6−23. (b) Burger, B. J.; Bercaw, J. E. In *Experimental Organometallic Chemistry*; Wayda, A. L., Darensbourg, M. Y., Eds.; American Chemical Society: Washington, DC, 1987; Chapter 4, pp 79−98. (c) Shriver, D. F.; Drezdzon, M. A. *The Manipulation of Air-Sensitive Compounds*, 2nd ed.; Wiley-Interscience: New York, 1986.

(25) Gottlieb, H. E.; Kotlyar, V.; Nudelman, A. *J. Org. Chem.* **1997**, *62*, 7512–7515.

(26) NMR Solvent Data Chart; Cambridge Isotope Laboratories, Inc.: Andover, MA, www.isotope.com/cil/products/images/nmrchart.pdf.

(27) Murphy, V. J.; Parkin, G. *J. Am. Chem. Soc.* **1995**, *117*, 3522–3528.

difference map techniques, and were refined by full-matrix least-squares procedures on F^2 with SHELXTL (Version 6.10).[28]

Computational Details. Calculations were carried out using DFT as implemented in the Jaguar 7.0 suite of *ab initio* quantum chemistry programs.[29] Geometry optimizations were performed with the B3LYP density functional[30] using the 6-31G** (C, H, N and P) and LACVP (Mo) basis sets.[31] The energies of the optimized structures were reevaluated by additional single-point calculations on each optimized geometry using cc-pVTZ(-f) correlation consistent triple-ζ basis set for C, H, N, and P and LACV3P for Mo (Table S2). Molecular orbital analyses were performed with the aid of Jimp 2,[32] which employs Fenske−Hall calculations[33] and visualization using MOPLOT.[34]

Synthesis of (η^6-C_6-PhzH)Mo(PMe$_3$)$_3$. A mixture of Mo(PMe$_3$)$_6$ (83 mg, 0.15 mmol) and phenazine (27 mg, 0.15 mmol) in benzene (*ca.* 0.7 mL) was heated at 80 °C for 4 h, after which period the volatile components were removed *in vacuo*. The residue was extracted into benzene (2 mL) and filtered. The filtrate was lyophilized,[35] and the resulting residue was washed with pentane (4 mL) and then dried *in vacuo* to give (η^6-C_6-PhzH)Mo(PMe$_3$)$_3$ as a green solid (65 mg, 86% yield) which contains a small amount of phenazine (<5%) and 5,10-dihydrophenazine (<3%). Crystals suitable for X-ray diffraction were grown by slow evaporation of a solution in pentane. Anal. Calcd. for $C_{21}H_{35}N_2P_3Mo$: C, 50.0%; H, 7.0%; N, 5.6%. Found: C, 50.0%; H, 6.8%; N, 5.4%. ^{1}H NMR (C_6D_6): 0.81 [br, 9H of 1 PMe$_3$], 1.01 [br, 18H of 2 PMe$_3$], 4.03 [s, 2H of PhzH], 5.24 [s, 2H of PhzH], 7.26 [m, 2H of PhzH], 8.06 [m, 2H of PhzH]. ^{13}C{^{1}H} NMR (C_6D_6): 23.7 [br, 6C of 2 PMe$_3$], 25.6 [br, 3C of 1 PMe$_3$], 71.0 [s, 2C of PhzH], 78.5 [s, 2C of PhzH], 124.0 [s, 2C of PhzH], 124.4 [s, 2C of PhzH], 126.7 [s, 2C of PhzH], 143.2 [s, 2C of PhzH]. ^{31}P{^{1}H} (C_6D_6): 2.4 [d, $^2J_{P-P}$ = 28, 2P of PMe$_3$], 17.5 [br, 1P of PMe$_3$]. IR Data (KBr disk, cm^{-1}): 3065 (m), 3050 (m), 2981 (m), 2959 (s), 2898 (s), 2802 (w), 1596 (w), 1529 (s), 1500 (m), 1470 (m), 1452 (vs), 1435 (s), 1420 (vs), 1378 (s), 1363 (m), 1334 (w), 1293 (m), 1276 (s), 1246 (s), 1141 (m), 1116 (m), 1074 (w), 1008 (vw), 984 (w), 954 (vs), 939 (vs), 928 (vs), 864 (m), 844 (m), 834 (s), 794 (s), 770 (m), 758 (vs), 717 (m), 703 (s), 660 (vs), 602 (s), 538 (vw), 498 (vw), 485 (w), 469 (m), 455 (vw), 448 (w), 438 (vw), 420 (vw).

Comparison of the Reactivity of Mo(PMe$_3$)$_6$ towards Phenazine and Acridine. Two NMR tubes equipped with J. Young valves containing (i) a mixture of Mo(PMe$_3$)$_6$ (10 mg, 0.02 mmol) and phenazine (5 mg, 0.03 mmol) and (ii) a mixture of Mo(PMe$_3$)$_6$ (10 mg, 0.02 mmol) and acridine (5 mg, 0.03 mmol) were treated with a solution of C_6D_6 (*ca.* 0.7 mL), containing a trace amount of mesitylene as an internal standard. The samples were heated at 80 °C and monitored by ^{1}H NMR spectroscopy, thereby demonstrating that the reaction of Mo(PMe$_3$)$_6$ with phenazine to form (η^6-C_6-PhzH)Mo(PMe$_3$)$_3$ ($t_{1/2} \approx 10$ min) is more facile than the corresponding reaction with acridine to form (η^6-C_6-AcrH)Mo(PMe$_3$)$_3$ ($t_{1/2} \approx 200$ min) under the same conditions.

Synthesis of (η^4-C_4-PhzH)$_2$Mo(PMe$_3$)$_2$. A mixture of Mo(PMe$_3$)$_6$ (20 mg, 0.04 mmol) and phenazine (20 mg, 0.11 mmol) in benzene (*ca.* 0.7 mL) was heated at 95 °C for 4 days, over which period red crystals were deposited. The crystals were isolated, washed with pentane (2 mL) and dried *in vacuo* to give (η^4-C_4-PhzH)$_2$Mo(PMe$_3$)$_2$ as a red solid (12 mg, 55% yield) suitable for X-ray diffraction. Anal. Calcd. for $C_{30}H_{34}N_4P_2Mo$: C, 59.2%; H, 5.6%; N, 9.2%. Found: C, 59.3%; H, 5.4%; N, 9.1%. ^{1}H NMR (C_6D_6): 0.42 [virtual triplet, PMe$_3$ (minor conformation)], 0.60 [d, $^2J_{P-H}$ = 7, PMe$_3$ (major conformation)], 2.97, 3.08, 3.21, 4.27, 4.82 [each broad singlet, 8H of 2 PhzH], 7.12 [m, 4H of 2 PhzH], 7.81 [m, 4H of 2 PhzH] (two conformations in the ratio 2:1 are observed in solution, but only the PMe$_3$ signals are distinct). IR Data (KBr disk, cm^{-1}): 3054 (w), 2964 (w), 2907 (w), 2851 (w), 1570 (w), 1506 (w), 1448 (w), 1410 (m), 1362 (vs), 1333 (m), 1287 (w), 1261 (w), 1217 (w), 1114 (w), 1018 (w), 948 (s), 808 (w), 759 (s), 714 (w), 668 (w).

Synthesis of (μ-η^6,η^6-PhzH)[Mo(PMe$_3$)$_3$]$_2$. A mixture of Mo(PMe$_3$)$_6$ (50 mg, 0.09 mmol) and phenazine (8 mg, 0.04 mmol) in d_{12}-cyclohexane (*ca.* 0.7 mL) was heated at 140 °C for 5 h, after which period the volatile components were removed *in vacuo*. The residue was washed with benzene (*ca.* 0.5 mL) and with pentane (*ca.* 1 mL). Benzene (*ca.* 0.5 mL) was added and the mixture was lyophilized to give (μ-η^6,η^6-PhzH)[Mo(PMe$_3$)$_3$]$_2$ as a dark yellow solid (20 mg, 54% yield) which contains a small amount of 5,10-dihydrophenazine (<5%). Crystals suitable for X-ray diffraction were grown by slow evaporation of a solution in pentane at −18 °C. ^{1}H NMR (C_6D_6): 1.17 [d, $^2J_{P-H}$ = 5, 54H of 6 PMe$_3$], 3.95 [s, 4H of PhzH], 4.98 [s, 4H of PhzH]. ^{13}C{^{1}H} NMR (C_6D_6): 25.7 [d, $^1J_{P-C}$ = 28, 18C of 6 PMe$_3$], 70.6 [s, 4C of PhzH], 75.5 [s, 4C of PhzH], 120.2 [s, 4C of PhzH (quaternary)]. ^{31}P{^{1}H} (C_6D_6): 10.08 [very br, PMe$_3$]. IR Data (KBr disk, cm^{-1}): 3058 (w), 2958 (m), 2895 (s), 2790 (w), 1506 (w), 1473 (w), 1452 (w), 1414 (m), 1362 (w), 1327 (w), 1315 (w), 1288 (w), 1271 (s), 1117 (w), 1080 (w), 939 (vs), 928 (vs), 869 (w), 831 (w), 778 (w), 691 (w), 649 (m).

Synthesis of (η^4-C_4-PhzH)Mo(PMe$_3$)$_3$H$_2$. A solution of (η^6-C_6-PhzH)Mo(PMe$_3$)$_3$ (10 mg) in C_6D_6 (*ca.* 0.7 mL) with mesitylene as an internal standard was placed in an NMR tube equipped with a J. Young valve and saturated with H_2 (1 atm), thereby resulting in a rapid color change (*ca.* 1 min) from green to orange-brown. The reaction was monitored by ^{1}H and ^{31}P NMR spectroscopy, thereby demonstrating the conversion to (η^4-C_4-PhzH)Mo(PMe$_3$)$_3$H$_2$ (>95%). The volatile components were removed by lyophilization giving an orange-brown solid and crystals suitable for X-ray diffraction were grown by slow evaporation of a solution in pentane at −18 °C. ^{1}H NMR (C_6D_6, room temperature): −3.91 [very br, 2H of MoH$_2$], 0.95 [br, 27H of 3 PMe$_3$], 3.08 [s, 2H of PhzH], 4.67 [s, 2H of PhzH], 7.09 [m, 2H of PhzH], 7.74 [m, 2H of PhzH]. ^{1}H NMR ($C_6D_5CD_3$ at 90 °C, hydride region only): −4.05 [q, $^2J_{P-H}$ = 45, 2H of MoH$_2$]. ^{1}H NMR ($C_6D_5CD_3$ at −70 °C, hydride region only), two species in the ratio *ca.* 2:1 are observed: −3.98 [t, $^2J_{P-H}$ = 42, 1H], −2.47 [dt, $^2J_{P-H}$ = 66, $^2J_{P-H}$ = 39, 1H] (major species); −8.69 [t, $^2J_{P-H}$ = 57, 1H], −3.68 [m, 1H] (minor species). ^{13}C{^{1}H} NMR (C_6D_6): 24.4 [d, $^1J_{C-P}$ = 25, 9C of 3 PMe$_3$], 60.4 [s, 2C of PhzH], 76.4 [s, 2C of PhzH], 125.5 [s, 2C of PhzH], 126.5 [s, 2C of PhzH (quaternary)], 141.0 [s, 2C of PhzH], 164.3 [s, 2C of PhzH (quaternary)]. ^{31}P{^{1}H} NMR (C_6D_6): 6.8 [br, PMe$_3$]. ^{31}P NMR ($C_6D_5CD_3$ at −70 °C), two species are observed: 3.6 [br, 1P], 5.1 [br, 1P], 16.4 [br, 1P] (major species); −5.0 [t, $^2J_{P-P}$ = 15, 1P], 5.4 [m, 2P] (minor species). IR Data (KBr disk, cm^{-1}): 3059 (m), 3029 (m), 2968 (s), 2904 (s), 2803 (m), 1832 (m) [ν(Mo−H)], 1789 (m), 1737 (s) [ν(Mo−H)], 1689 (w), 1605 (w), 1567 (m), 1503 (s), 1480 (s), 1452 (s), 1414 (vs), 1358 (vs), 1300 (s), 1280 (vs), 1112 (m), 1100 (m), 1044 (vw), 1021 (vw), 941 (vs), 855 (s), 824 (m), 797 (m), 754 (vs), 720 (s), 709 (s), 667 (vs), 604 (s), 588 (s), 570 (m), 496 (s), 470 (m).

(28) (a) Sheldrick, G. M. *SHELXTL, An Integrated System for Solving, Refining and Displaying Crystal Structures from Diffraction Data*; University of Göttingen: Göttingen, Federal Republic of Germany, 1981. (b) Sheldrick, G. M. *Acta Crystallogr.* **2008**, *A64*, 112–122.
(29) *Jaguar 7.0*; Schrödinger, LLC: New York, NY, 2007.
(30) (a) Becke, A. D. *J. Chem. Phys.* **1993**, *98*, 5648–5652. (b) Becke, A. D. *Phys. Rev. A* **1988**, *38*, 3098–3100. (c) Lee, C. T.; Yang, W. T.; Parr, R. G. *Phys. Rev. B* **1988**, *37*, 785–789. (d) Vosko, S. H.; Wilk, L.; Nusair, M. *Can. J. Phys.* **1980**, *58*, 1200–1211. (e) Slater, J. C. *The Self-Consistent Field for Molecules and Solids*; Quantum Theory of Molecules and Solids, Vol. 4; McGraw-Hill: New York, 1974.
(31) (a) Hay, P. J.; Wadt, W. R. *J. Chem. Phys.* **1985**, *82*, 270–283. (b) Wadt, W. R.; Hay, P. J. *J. Chem. Phys.* **1985**, *82*, 284–298. (c) Hay, P. J.; Wadt, W. R. *J. Chem. Phys.* **1985**, *82*, 299–310.
(32) Manson, J. M. B.; Webster, C. E.; Hall, M. B. *Jimp 2, Version 0.089*; Department of Chemistry, Texas A&M University: College Station, TX 77842, 2006; http://www.chem.tamu.edu/jimp2.
(33) Hall, M. B.; Fenske, R. F. *Inorg. Chem.* **1972**, *11*, 768–775.
(34) Lichtenberger, D. L. *MOPLOT, Version 2.0*; Department of Chemistry, University of Arizona: Tuscon, AZ 85721, 1993.
(35) The sample was lyophilized by freezing the benzene solution in liquid N_2 and allowing the frozen sample to reach ambient temperature during the lyophilization process.

Synthesis of (μ-η^6,η^4-PhzH)[Mo(PMe$_3$)$_3$][Mo(PMe$_3$)$_3$H$_2$]. A solution of (μ-η^6,η^6-PhzH)[Mo(PMe$_3$)$_3$]$_2$ (5 mg) in C_6D_6 (*ca.* 0.7 mL) with mesitylene as an internal standard was placed in an NMR tube equipped with a J. Young valve and saturated with H_2 (1 atm). The reaction was monitored by ^{1}H NMR spectroscopy, thereby demonstrating the conversion to (μ-η^6,η^4-PhzH)[Mo(PMe$_3$)$_3$]-[Mo(PMe$_3$)$_3$H$_2$] (>95%) over a period of 30 min. The volatile components were removed by lyophilization giving a green solid and crystals suitable for X-ray diffraction were grown by slow evaporation of a solution in pentane at −18 °C. ^{1}H NMR (C_6D_6): −3.67 [br, 2H of MoH$_2$)] 1.00 [d, $^2J_{P-H}$ = 7, 27H of PMe$_3$], 1.37 [s, 27H of PMe$_3$], 2.97 [br, 2H of PhzH], 3.87 [br, 2H of PhzH], 4.65 [br, 2H of PhzH], 4.76 [br, 2H of PhzH]. ^{1}H NMR ($C_6D_5CD_3$ at −73 °C, hydride region only), two species in the ratio *ca.* 2.5:1 are observed: −4.03 [t, $^2J_{P-H}$ = 41, 1H], −2.59 [dt, $^2J_{P-H}$ = 66, $^2J_{P-H}$ = 40, 1H] (major species); −8.30 [t, $^2J_{P-H}$ = 54, 1H], −3.75 [m, 1H] (minor species). ^{13}C{^{1}H} NMR (C_6D_6): 24.7 [d,$^1J_{P-C}$ = 24, 9C of PMe$_3$], 26.9 [m, 9C of PMe$_3$], 60.2 [s, 2C of PhzH], 70.0 [s, 2C of PhzH], 72.4 [s, 2C of PhzH], 74.6 [s, 2C of PhzH], 102.0 [s, 2C of PhzH], 159.4 [s, 2C of PhzH]. ^{31}P{^{1}H} (C_6D_6): 7.1 [br, 6 P of PMe$_3$]. IR Data (KBr disk, cm^{-1}): 3046 (w), 3018 (w), 2957 (m), 2896 (s), 2797 (w), 1739 (br, m), 1556 (w), 1510 (m), 1418 (m), 1383 (w), 1361 (w), 1332 (m), 1280 (m), 1193 (w), 1097 (w), 1067 (w), 942 (vs), 845 (m), 718 (w), 689 (w), 657 (m).

Reactivity of (η^4-*C*$_4$-PhzH)$_2$Mo(PMe$_3$)$_2$ towards H_2. (a) A suspension of (η^4-*C*$_4$-PhzH)$_2$Mo(PMe$_3$)$_2$ (10 mg) in C_6D_6 (*ca.* 0.7 mL) was placed in an NMR tube equipped with a J. Young valve and saturated with H_2 (*ca.* 1 atm). The sample was left at room temperature and monitored by ^{1}H NMR spectroscopy, thereby demonstrating that (η^4-*C*$_4$-PhzH)$_2$Mo(PMe$_3$)$_2$ did not react after 2 days.

(b) A suspension of (η^4-*C*$_4$-PhzH)$_2$Mo(PMe$_3$)$_2$ (10 mg) in C_6D_6 (*ca.* 0.7 mL) was placed in an NMR tube equipped with a J. Young valve and saturated with H_2 (*ca.* 1 atm). The sample was heated at 95 °C and monitored by ^{1}H NMR spectroscopy, thereby demonstrating that (η^4-*C*$_4$-PhzH)$_2$Mo(PMe$_3$)$_2$ remained largely unreacted after 5 days.

Synthesis of (η^4-*C*$_4$-AcrH)Mo(PMe$_3$)$_3$H$_2$. A solution of (η^6-*C*$_6$-AcrH)Mo(PMe$_3$)$_3$ (10 mg) in C_6D_6 (*ca.* 0.7 mL) with mesitylene as an internal standard was placed in an NMR tube equipped with a J. Young valve and saturated with H_2 (1 atm), thereby resulting in a rapid color change (*ca.* 30 min) from green to yellow. The reaction was monitored by ^{1}H and ^{31}P NMR spectroscopy, thereby demonstrating the conversion to (η^4-*C*$_4$-AcrH)Mo(PMe$_3$)$_3$H$_2$ (>95%). The volatile components were removed by lyophilization giving a yellow solid and crystals suitable for X-ray diffraction were grown by slow evaporation of a solution in pentane at −18 °C. ^{1}H NMR (C_6D_6): −4.0 [very br, 2H of MoH$_2$], 0.99 [d, $^2J_{P-H}$ = 7, 27H of PMe$_3$], 2.68 [br, 1H of AcrH], 3.10 [br, 1H of AcrH], 4.73 [br, 1H of AcrH], 4.78 [br, 1H of AcrH], 6.58 [s, 1H of AcrH], 7.05 [t, $^3J_{H-H}$ = 8, 1H of AcrH], 7.17 [t, $^3J_{H-H}$ = 8, 1H of AcrH], 7.21 [d, $^3J_{H-H}$ = 8, 1H of AcrH], 7.97[d, $^3J_{H-H}$ = 8, 1H of AcrH]. ^{1}H NMR ($C_6D_5CD_3$ at 90 °C, hydride region only): −3.92 [q, $^2J_{P-H}$ = 47, 2H of MoH$_2$)]. ^{1}H NMR ($C_6D_5CD_3$ at −70 °C, hydride region only), two species in the ratio *ca.* 3:1 are observed: −4.03 [t, $^2J_{P-H}$ = 41, 1H], −2.39 [dt, $^2J_{P-H}$ = 61,$^2J_{P-H}$ = 43, 1H] (major species); −8.54 [t, $^2J_{P-H}$ = 56, 1H], −3.68 [m, 1H] (minor species). The T_1 minimum values of the hydride signals of the major species in toluene-d_8 are 243 ms (δ −4.03 ppm) and 203 ms (δ −2.39 ppm) at 300 MHz and −60 °C. ^{13}C{^{1}H} NMR (C_6D_6): 24.5 [d, $^1J_{P-C}$ = 24, 9C of PMe$_3$], 55.0 [s, 1C of AcrH], 62.2 [s, 1C of AcrH], 75.4 [s, 1C of AcrH], 77.0 [s, 1C of AcrH], 119.2 [s, 1C of AcrH (quaternary)], 123.6 [s, 1C of AcrH (quaternary)], 125.2 [s, 1C of AcrH], 125.8 [s, 1C of AcrH (quaternary)], 127.5 [s, 1C of AcrH], 142.8 [s, 1C of AcrH], 146.2 [s, 1C of AcrH], 170.9 [s, 1C of AcrH], 1C not observed. ^{31}P{^{1}H} NMR (C_6D_6): 6 [very br, 3P of PMe$_3$]. ^{31}P NMR ($C_6D_5CD_3$ at −70 °C): ABC pattern, 4.75 [$^2J_{P-P}$ = 23, $^2J_{P-P}$ = 26], 5.70 [$^2J_{P-P}$ = 23, $^2J_{P-P}$ = 27], 15.48 [$^2J_{P-P}$ = 26, $^2J_{P-P}$ = 27]. IR data (KBr disk, cm^{-1}): 3046 (m), 2965 (s), 2902 (s), 2802 (m), 1740 (m) [ν(Mo−H)], 1722 (m) [ν(Mo−H)], 1604 (m), 1582 (m), 1560 (s), 1519 (m), 1470 (m), 1437 (s), 1418 (s), 1385 (vs), 1321 (s), 1298 (s), 1277 (s), 1226 (s), 1142 (w), 1114 (w), 1096 (w), 1037 (vw), 1024 (vw), 940 (vs), 848 (s), 787 (m), 748 (s), 714 (s), 664 (vs), 613 (s), 585 (s), 518 (m), 490 (m), 462 (m).

Synthesis of (η^4-*C*$_4$-QoxH)Mo(PMe$_3$)$_3$H$_2$. A solution of (η^6-*C*$_6$-QoxH)Mo(PMe$_3$)$_3$ (10 mg) in C_6D_6 (*ca.* 0.7 mL) with mesitylene as an internal standard was placed in an NMR tube equipped with a J. Young valve and saturated with H_2 (*ca.* 1 atm). The reaction was monitored by ^{1}H NMR spectroscopy, thereby demonstrating the conversion to an equilibrium mixture with (η^4-*C*$_4$-QoxH)Mo-(PMe$_3$)$_3$H$_2$ over a period of 2 days ($K = 7.2 \times 10^2$ M^{-1} at room temperature). Crystals suitable for X-ray diffraction were grown by slow evaporation of a solution in pentane at −18 °C. ^{1}H NMR (C_6D_6): −4.0[very br, 2H of MoH$_2$], 1.01 [d, $^2J_{P-H}$ = 7, 27H of PMe$_3$], 2.75 [s, 2H of QoxH], 4.83 [s, 2H of QoxH], 7.26 [s, 2H of QoxH]. ^{1}H NMR ($C_6D_5CD_3$ at −73 °C, hydride region only), two species in the ratio *ca.* 3:1 are observed: −3.89 [ddt, $^2J_{P-H}$ = 41, $^2J_{P-H}$ = 10, $^2J_{H-H}$ = 10, 1H], −2.42 [dt, $^2J_{P-H}$ = 67,$^2J_{P-H}$ = 39, 1H] (major species); −8.64 [ddt, $^2J_{P-H}$ = 57, $^2J_{P-H}$ = 11, $^2J_{H-H}$ = 11, 1H], −3.61 [m, 1H] (minor species).

Structural Characterization of (η^4-AnH)Mo(PMe$_3$)$_3$H$_2$. (η^4-AnH)Mo(PMe$_3$)$_3$H$_2$ was synthesized as previously reported[6] *via* reaction of (η^6-AnH)Mo(PMe$_3$)$_3$ with H_2, and crystals suitable for X-ray diffraction were obtained by slow evaporation of a pentane solution at −18 °C.

Hydrogenation of (η^6-*C*$_6$-PhzH)Mo(PMe$_3$)$_3$. A solution of (η^6-*C*$_6$-PhzH)Mo(PMe$_3$)$_3$ (5 mg) in C_6D_6 (*ca.* 0.7 mL) with mesitylene as an internal standard was placed in an NMR tube equipped with a J. Young valve and saturated with H_2 (*ca.* 1 atm), thereby resulting in a color change from green to orange-brown over a period of *ca.* 1 min due to the formation of (η^4-*C*$_4$-PhzH)Mo(PMe$_3$)$_3$H$_2$. The solution was then heated at 95 °C for 17 days and monitored by ^{1}H NMR spectroscopy, thereby demonstrating conversion to, *inter alia*, 5,10-dihydrophenazine[36] (*ca.* 50%) and 1,2,3,4-tetrahydrophenazine[37] (*ca.* 30%). The principal molybdenum-containing species produced is (η^6-*d*$_6$-PhH)Mo(PMe$_3$)$_3$ (*ca.* 70%), together with trace amounts of (η^4-*C*$_4$-PhzH)$_2$Mo(PMe$_3$)$_2$.

Hydrogenation of (η^6-*C*$_6$-AcrH)Mo(PMe$_3$)$_3$. A solution of (η^6-*C*$_6$-AcrH)Mo(PMe$_3$)$_3$ (5 mg) in C_6D_6 (*ca.* 0.7 mL) with mesitylene as an internal standard was placed in an NMR tube equipped with a J. Young valve and saturated with H_2 (*ca.* 1 atm), thereby resulting in a color change from green to yellow over a period of *ca*. 30 min due to the formation of (η^4-*C*$_4$-AcrH)Mo(PMe$_3$)$_3$H$_2$. The solution was heated at 95 °C for 3 days and monitored by ^{1}H NMR spectroscopy, thereby demonstrating conversion to 9,10-dihydroacridine (*ca.* > 95%), which was identified by comparison of the ^{1}H NMR spectrum in $CDCl_3$ with that of an authentic sample.[38] The principal molybdenum-containing species produced is (η^6-*d*$_6$-PhH)Mo(PMe$_3$)$_3$.

Internal Comparison of the Reactivity of (η^6-*C*$_6$-AcrH)Mo-(PMe$_3$)$_3$ and (η^6-*C*$_6$-QH)Mo(PMe$_3$)$_3$ toward H_2. A solution of (η^6-*C*$_6$-AcrH)Mo(PMe$_3$)$_3$ (5 mg) and (η^6-*C*$_6$-QH)Mo(PMe$_3$)$_3$ (5 mg) in C_6D_6 (*ca.* 0.7 mL) with mesitylene as an internal standard was placed in an NMR tube equipped with a J. Young valve and saturated with H_2 (*ca.* 1 atm). The solution was heated at 95 °C and monitored by ^{1}H NMR spectroscopy, thereby demonstrating that (η^6-*C*$_6$-AcrH)Mo(PMe$_3$)$_3$ released 9,10-dihydroacridine over a period of 3 days, while (η^6-*C*$_6$-QH)Mo(PMe$_3$)$_3$ was stable with respect to hydrogenation over this period, although a small amount

(36) (a) Sugimoto, A.; Kotani, T.; Tsujimoto, J.; Yoneda, S. *J. Heterocycl. Chem.* **1989**, *26*, 435–438. (b) Bettinetti, G. F.; Maffei, S.; Pietra, S. *Synthesis* **1976**, 748–749.

(37) The formation of 1,2,3,4-tetrahydrophenazine was confirmed by removing all volatile components and recording the spectrum in $CDCl_3$ and comparing it with the literature data. See: Petukhov, P. A.; Tkachev, A. V. *Tetrahedron* **1997**, *53*, 9761–9768.

of quinoline (*ca.* 25 %) dissociates due to conversion to (η^6-d_6-PhH)Mo(PMe_3)$_3$.

Hydrogenation of Acridine in the Presence of (η^6-C_6-AcrH)Mo(PMe_3)$_3$. A solution of (η^6-C_6-AcrH)Mo(PMe_3)$_3$ (4 mg) and acridine (7.4 equiv) in d_{12}-cyclohexane (*ca.* 0.7 mL) with mesitylene as an internal standard was placed in an NMR tube equipped with a J. Young valve and saturated with H_2 (*ca.* 1 atm), thereby resulting in a change in color from green to yellow over a period of *ca.* 30 min, indicating the conversion to (η^4-C_4-AcrH)Mo(PMe_3)$_3H_2$. The solution was heated at 95 °C and monitored by ^{1}H NMR spectroscopy, thereby demonstrating the catalytic hydrogenation of 7.2 equiv of acridine (in addition to the coordinated acridine) over a period of 21 days to a mixture of 9,10-dihydroacridine[38] and 1,2,3,4-tetrahydroacridine,[39] which were identified by ^{1}H NMR spectroscopy and mass spectrometry. Due to solubility differences in cyclohexane, the ratio of 9,10-dihydroacridine to 1,2,3,4-tetrahydroacridine (2:3) was determined by ^{1}H NMR spectroscopic analysis of the product mixture in $CDCl_3$. In addition to 9,10-dihydroacridine and 1,2,3,4-tetrahydroacridine, a small amount of insoluble 9,9′-biacridane was identified by X-ray diffraction. The latter compound has been reported to be generated *via* reaction between acridine and 9,10-dihydroacridine.[40] The hydrogenation reaction was repeated in the presence of elemental Hg, which was found to have no impact on the course of the reaction.

Measurement of the Equilibrium Constant for Oxidative Addition of H_2 to (η^6-C_6-QoxH)Mo(PMe_3)$_3$. A solution of (η^6-C_6-QoxH)Mo(PMe_3)$_3$ (5 mg) C_6D_6 (*ca.* 0.7 mL) with mesitylene as an internal standard was placed in an NMR tube equipped with a J. Young valve and saturated with H_2 (1 atm). The reaction was monitored by ^{1}H NMR spectroscopy, thereby demonstrating the conversion to an equilibrium mixture with (η^4-C_4-QoxH)Mo(PMe_3)$_3H_2$ over a period 2 days ($K = 7.2 \times 10^2$ M^{-1} at room temperature). The concentration of H_2 was determined using reported solubility data.[41]

Measurement of the Equilibrium Constant for H_2 Transfer from (μ-η^6,η^4-PhzH)[Mo(PMe_3)$_3$][Mo(PMe_3)$_3H_2$] to (η^6-C_6-PhzH)Mo(PMe_3)$_3$. A solution of (μ-η^6,η^4-PhzH)[Mo(PMe_3)$_3$][Mo(PMe_3)$_3$-H_2] (7 mg, 0.008 mmol) and (η^6-C_6-PhzH)Mo(PMe_3)$_3$ (4 mg, 0.008 mmol) in C_6D_6 (*ca.* 0.7 mL) with mesitylene as an internal standard was placed in an NMR tube equipped with a J. Young valve. The sample was placed in a constant temperature bath at 30 °C and monitored for several days by ^{1}H NMR spectroscopy, thereby demonstrating the transfer of H_2 from (μ-η^6,η^4-PhzH)[Mo(PMe_3)$_3$]-[Mo(PMe_3)$_3H_2$] to (η^6-C_6-PhzH)Mo(PMe_3)$_3$, producing (μ-η^6,η^6-PhzH)[Mo(PMe_3)$_3$]$_2$ and (η^4-C_4-PhzH)Mo(PMe_3)$_3H_2$ as components of an equilibrium mixture ($K = 7.4$).

Measurement of the Equilibrium Constant for H_2 Transfer from (η^4-AnH)Mo(PMe_3)$_3H_2$ to (η^6-C_6-AcrH)Mo(PMe_3)$_3$. A solution of (η^4-AnH)Mo(PMe_3)$_3H_2$ (5 mg) and (η^6-C_6-AcrH)Mo(PMe_3)$_3$ (5 mg) in C_6D_6 (*ca.* 0.7 mL) with mesitylene as an internal standard was placed in an NMR tube equipped with a J. Young valve. The sample was placed in a constant temperature bath at 30 °C and monitored for several days by ^{1}H NMR spectroscopy, thereby demonstrating the transfer of H_2 from (η^4-AnH)Mo(PMe_3)$_3H_2$ to (η^6-C_6-AcrH)Mo(PMe_3)$_3$, producing (η^6-AnH)Mo(PMe_3)$_3$ and (η^4-C_4-AcrH)Mo(PMe_3)$_3H_2$ as components of an equilibrium mixture ($K = 2.0$).

Measurement of the Equilibrium Constant for H_2 Transfer from (η^4-C_4-AcrH)Mo(PMe_3)$_3H_2$ to (η^6-C_6-PhzH)Mo(PMe_3)$_3$. A solution of (η^4-C_4-AcrH)Mo(PMe_3)$_3H_2$ (5 mg) and (η^6-C_6-PhzH)-Mo(PMe_3)$_3$ (5 mg) in C_6D_6 (*ca.* 0.7 mL) with mesitylene as an internal standard was placed in an NMR tube equipped with a J. Young valve. The sample was placed in a constant temperature bath at 30 °C and monitored for several days by ^{1}H NMR spectroscopy, thereby demonstrating the transfer of H_2 from (η^4-C_4-AcrH)Mo(PMe_3)$_3H_2$ to (η^6-C_6-PhzH)Mo(PMe_3)$_3$, producing (η^6-C_6-AcrH)Mo(PMe_3)$_3$ and (η^4-C_4-PhzH)Mo(PMe_3)$_3H_2$ as components of an equilibrium mixture ($K = 1.8 \times 10^2$).

Computational Analysis of Oxidative Addition of H_2 to (η^6-NHetH)Mo(PMe_3)$_3$. A computational analysis of the oxidative addition of H_2 to (η^6-NHetH)Mo(PMe_3)$_3$ giving (η^4-NHetH)Mo-(PMe_3)$_3H_2$ was performed for a computationally simpler system in which the methyl groups of the PMe_3 ligands were replaced by hydrogen atoms. Furthermore, in each case, two isomers of (η^4-NHetH)Mo(PH_3)$_3H_2$ were considered on the basis of the X-ray diffraction and ^{1}H NMR spectroscopic studies on (η^4-NHetH)Mo(PMe_3)$_3H_2$. The thermodynamics for formation of both isomers of (η^4-NHetH)Mo(PH_3)$_3H_2$ by oxidative addition of H_2 to (η^6-NHetH)Mo(PH_3)$_3$ were evaluated. Significantly, for each isomer, the calculations (Table 2) indicate that oxidative addition of H_2 becomes more exothermic in the sequence anthracene < acridine < phenazine, in accord with experimental observations.

Acknowledgment. We thank the U.S. Department of Energy, Office of Basic Energy Sciences (DE-FG02-93ER14339) for support of this research. The National Science Foundation (CHE-0619638) is thanked for acquisition of an X-ray diffractometer. Daniela Buccella and Philip May (NSF REU program) are thanked for helpful contributions.

Supporting Information Available: Tables of crystallographic data, CIF files and Cartesian coordinates for geometry optimized structures. This material is available free of charge *via* the Internet at http://pubs.acs.org.

JA901896X

(38) Srikrishna, A.; Reddy, T. J.; Viswajanani, R. *Tetrahedron* **1996**, *52*, 1631–1636.
(39) Banwell, M. G.; Lupton, D. W.; Ma, X.; Renner, J.; Sydnes, M. O. *Org. Lett.* **2004**, *6*, 2741–2744.
(40) (a) Takano, J.; Kitahara, T.; Shihara, Y.; Shirai, K. *Proc. Fac. Sci. Tokai Univ.* **1985**, *20*, 111–116. (b) Takano, J.; Kitahara, T.; Shihara, Y.; Shirai, K. *Nippon Kagaku Kaishi* **1983**, 400–404.
(41) Clever, H. L. In *Hydrogen and Deuterium Solubility Tables*; Young, C. L., Ed.; Solubility Data Series, *Volume 5/6*; Pergamon Press: Oxford, 1981; p 159.